JOURNAL OF Materials CHEMISTRY

# Homogeneous polymer–zeolite nanocomposite membranes by incorporating dispersible template-removed zeolite nanocrystals

**Huanting Wang, Brett A. Holmberg and Yushan Yan***

*Department of Chemical and Environmental Engineering, University of California, Riverside, California 92521, USA. E-mail: yushan.yan@ucr.edu*

***Received 29th July 2002, Accepted 24th September 2002***
***First published as an Advance Article on the web 18th October 2002***

Homogeneous polymer–zeolite membranes were fabricated by incorporation of dispersible template-removed zeolite A nanocrystals into polysulfone. SEM, XRD, $N_2$ adsorption–desorption measurements were used to characterize the zeolite A nanocrystals. The uniformity of the polysulfone–zeolite A nanocomposite membranes was examined by SEM. Air separation measurements of the nanocomposite membranes showed enhanced performance in $O_2/N_2$ selectivity and $O_2$ permeability. The polysulfone–zeolite nanocomposite membrane with 25 wt% zeolite A loading exhibited an $O_2/N_2$ selectivity of 7.7 and $O_2$ permeability of 1.8 Barrers whereas the pure polysulfone membrane had an $O_2/N_2$ selectivity of 5.9 and $O_2$ permeability of 1.3 Barrers.

## 1. Introduction

Polymeric membranes are becoming increasingly important for gas separations because they are relatively inexpensive and can be fabricated into compact hollow fiber modules with very high separation area to volume ratio.[1–3] One of the important separations for polymer membranes is air separation. However, polymeric membranes usually have low $O_2/N_2$ selectivity, significantly limiting their widespread applications. Zeolites are microporous crystalline aluminosilicates with uniform molecular-sized pores and have been used in powder composite form as molecular sieving separation media. Theory has predicted that incorporation of zeolite 4A crystals into a polymer matrix could significantly improve its $O_2/N_2$ selectivity.[4] This kind of polymer–zeolite composite membrane is sometimes called a mixed-matrix membrane.[4] Successful preparation of polymer–zeolite composite membranes requires solving material selection and defect elimination problems.[5] By carefully selecting a polymer matrix to avoid interfacial incompatibility and defects between the zeolite crystals and polymer matrix, polymer–zeolite composite membranes (*e.g.*, PVA–zeolite 4A) were shown to have higher $O_2/N_2$ selectivity than the parent matrix polymer.[5]

At present, most of the studies on composite membranes use rather large zeolite particles that are commercially available (*e.g.*, micrometer). However, polymeric membranes are usually shaped into asymmetric hollow fibers with a thin (*e.g.*, 100 nm) selective layer for practical applications. Thus large zeolite crystals are not suitable for developing pratical composite membranes. Apparently zeolite nanocrystals are required for this purpose. There have been numerous publications on the synthesis of colloidal zeolite nanocrystals.[6–8] As-synthesized zeolite nanocrystals usually contain an organic template inside their pores. Template-free zeolite nanocrystals are required for the purpose of membrane applications. Thus far, the most commonly used method for template removal is through high temperature calcination (*e.g.*, 500 °C). This method has proven unsuitable for colloidal zeolite nanocrystals because it leads to severe irreversible aggregation, and non-homogeneous dispersion of zeolite in polymer.[9] Very recently we have developed a novel technique for the preparation of dispersible template-removed zeolite nanocrystals in various solvents by using an organic polymer network as a temporary barrier during calcination to prevent zeolite nanocrystal aggregation.[10] This newly developed technique is used here for preparing dispersible template-removed zeolite nanocrystals.

In this paper, we attempt to develop homogeneous polymer–zeolite nanocomposite membranes for air separation. A commonly used air separation membrane material, polysulfone[1–3,11–13] is chosen as the polymer matrix, and zeolite A nanocrystals as the additive. Zeolite 4A–polysulfone composite membranes have been predicted to be commercially attractive for $O_2/N_2$ separation.[4] Both small particle size and good dispersibility of zeolite 4A nanocrystals are expected to improve interfacial compatibility between zeolite 4A nanocrystals and polysulfone, and thus enhance $O_2/N_2$ selectivity. Zeolite 4A refers to $Na^+$ exchanged zeolite A with a Si : Al ratio of 1. Zeolite 4A crystals are normally synthesized in the $Na_2O$–$SiO_2$–$Al_2O_3$–$H_2O$ system without using any organic template. However, without a template, the $Na_2O$–$SiO_2$–$Al_2O_3$–$H_2O$ system usually produces crystals larger than 500 nm.[14] Here we synthesize zeolite A with TMAOH to produce nanocrystals since this synthetic approach is well established.[15–19] It is noted however that TMA-synthesized zeolite A usually has a Si : Al ratio higher than 1 and has a pore size of 4.3 Å, which is slightly larger than zeolite 4A (4.0 Å).[19] To the best of our knowledge, this is the first report on the fabrication and study of air separation properties of polysulfone–dispersible zeolite A nanocrystal composite membranes.

## 2. Experimental

### 2.1. Synthesis of zeolite A nanocrystals

Zeolite A nanocrystals were synthesized by hydrothermal synthesis from a clear solution with a composition of 1.00 $Al_2O_3$ : 6.12 $SiO_2$ : 7.17 $(TMA)_2O$ : 0.16 $Na_2O$ : 345 $H_2O$.[16] The solution for synthesis was prepared in a 250 mL polypropylene bottle. First, aluminium isopropoxide (Aldrich) was dissolved in a solution made from 25 wt% aqueous tetramethylammonium hydroxide (TMA, Aldrich), 97 wt% sodium hydroxide (EM Science), and doubly distilled water. Once the solution became clear, Ludox HS-30 colloidal silica (Aldrich) was added to begin a two-day aging process. Strong magnetic stirring was maintained during aging. The solution was then heated in a silicone oil temperature bath with stirring at 100 °C for two days. The solid product contained in the colloidal suspension was recovered by a repeated cycle of

DOI: 10.1039/b207394c

two-hour centrifugation at 48000*g*, careful decanting, and ultrasonic redispersion in water until pH $< 8$ to form colloidal zeolite A–water suspension.

### 2.2. Template-removal and sodium exchange of zeolite A nanocrystals

In order to remove TMA without nanocrystal aggregation, a polymer network was introduced into the colloidal zeolite A–water suspension.[10] Organic monomer acrylamide ($CH_2$=CHCONH$_2$, AM, Aldrich) and crosslinker *N*,*N*′-methylenebisacrylamide ($CH_2$=CHCONH)$_2$CH$_2$, MBAM, Aldrich), and initiator $(NH_4)_2S_2O_8$ (Aldrich) were added to the nanocrystal suspension in water. Typically, 1.0 g AM, 0.1 mg MBAM and 25 mg $(NH_4)_2S_2O_8$ were added under stirring to 10 g of zeolite A colloidal suspension with *ca.* 5 wt% solid loading. After the monomer had dissolved, the mixture was ultrasonicated for 15 minutes to ensure complete dispersion of zeolite A nanocrystals. The monomer aqueous solution has a fairly low viscosity and was readily polymerized and crosslinked free-radically into an elastic hydrogel once the temperature was increased to 50 °C or a catalyst *N*,*N*,*N*′,*N*′-tetramethylethylenediamine was added at room temperature. The solid polymer–zeolite A composite was dried at 80–100 °C overnight before it was carbonized under nitrogen at 500 °C for 2 hours (heating rate 2 °C min$^{-1}$). In order to reduce the pore window size of zeolite A, the zeolite A–carbon composites were treated with a 10 wt% $NaNO_3$ aqueous solution at 80 °C for 10 h to allow sodium ion exchange, followed by washing with deionized water, and calcination at 500 °C for 4 h under oxygen to completely remove carbon and possible $NO_3^-$ residues. The obtained cotton-like zeolite A nanocrystals were easily dispersed into many solvents. These dispersible zeolite A nanocrystals were denoted as D–A. As a comparison, some as-synthesized zeolite A nanocrystals were directly calcined without going through the polymer network procedure followed by sodium exchange under identical conditions to D–A, and the product obtained were denoted as C–A.

### 2.3. Preparation of polysulfone–zeolite A nanocomposite membranes

The preparation flowchart of polysulfone (PSF)–zeolite A nanocomposite membranes is shown in Fig. 1. Polysulfone (Udel, BP-AMOCO) beads were dissolved in *N*-methyl-2-pyrrolidinone (NMP, 99%, Aldrich) at room temperature for 1 day to make 8 wt% polysulfone in NMP solution. A measured amount of zeolite A nanocrystals were then added, and the resultant suspension was ultrasonicated for 30 minutes to ensure good dispersion of zeolite nanocrystals. The polysulfone solutions with zeolite loading of 0, 15, 25, 30, 35 wt% (based on weight of polysulfone) were cast on a silicon wafer, and dried at 90 °C overnight to obtain the final polysulfone–zeolite A nanocomposite membranes. The membranes were around 60 μm thick, measured with a micrometer, and cut into small pieces with a diameter of 2.0 cm for gas separation measurements.

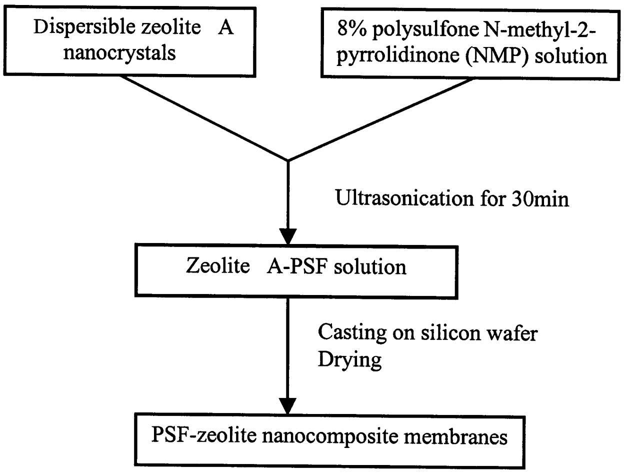

**Fig. 1** Preparation flowchart of polysulfone (PSF)–zeolite A nanocomposite membranes.

### 2.4 Characterization methods

X-Ray diffraction (Siemens D-500 diffractometer using Cu-Kα radiation) was used to confirm zeolite A structures. Elemental analyses of as-synthesized and sodium exchanged zeolite A nanocrystals were carried out by Galbraith Laboratories, Inc. Thermogravimetric (TG, Cahn D-200) analysis of the as-synthesized sample was carried out at 10 °C min$^{-1}$ in air and was used to observe water content and the decomposition of TMA in the zeolite A framework. The as-synthesized zeolite A nanocrystals retrieved from the synthesis solution were dried at 80 °C overnight prior to TG analysis.

Nitrogen adsorption–desorption measurements were carried out at −196 °C on a Micromeritics ASAP 2010 instrument to determine Brunaer–Emmett–Teller (BET) surface area and micropore volume. Before measurements were taken, samples were evacuated overnight at 350 °C and 1 μmHg. The zeolite nanocrystals and nanocomposite membranes were examined with a scanning electron microscope (SEM, Philips XL30-FEG operating at 5 kV).

To test air separation properties, the membrane samples were attached to a glass holder using Torr Seal® epoxy resin (Varian). Before measurements were taken, the samples were evacuated under a vacuum of 1 μmHg at 90 °C for 1–2 days to remove any residual solvent and adsorbed water. The feed air flowed continuously outside of the membrane at 1 atm while the inside was swept by helium at 1 atm. Permeation experiments were carried out at room temperature. The composition of the feed and the permeate streams were measured using a SRI 8610C gas chromatograph equipped with a thermal conductivity detector (TCD) and a molecular sieve column. The permeate gas composition yields permeability $P_i$ , which is defined as $P_i = (dN_i)/(\Delta P_i A)$, where $d$ is the membrane thickness (cm), $N_i$ the permeation rate of component i (cm$^3$ s$^{-1}$), $\Delta P_i$ the transmembrane pressure difference of i (cmHg), and $A$ the membrane area (cm$^2$). 1 Barrer $= 10^{-10}$ cm$^3$(STP) cm cm$^{-2}$ s$^{-1}$ cmHg$^{-1}$. The selectivity $S_{ij}$ is defined as: $S_{ij} = P_i/P_j$.

## 3. Results and discussion

### 3.1. Zeoilte A nanocrystals

The SEM image of as-synthesized zeolite A nanocrystals is shown in Fig. 2. Zeolite A nanocrystals exhibit a wide particle

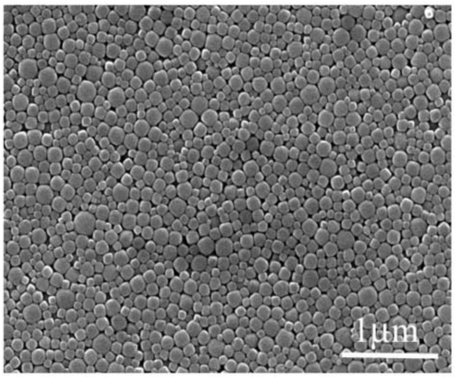

**Fig. 2** SEM image of as-synthesized zeolite A nanocrystals.

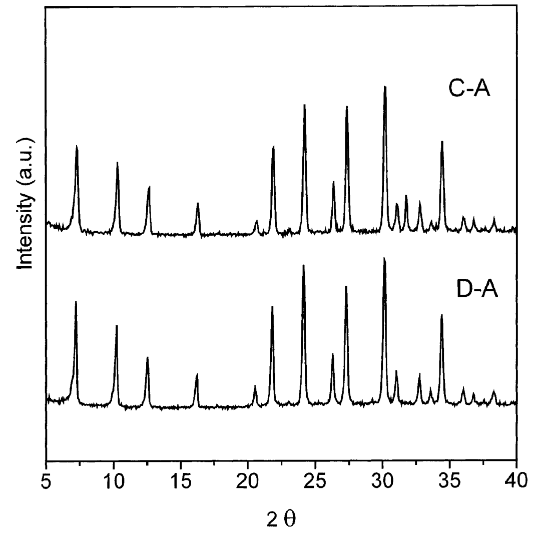

**Fig. 3** XRD patterns of zeolite A nanocrystals. Sample D–A was prepared by polymer network and sodium exchange; sample C–A was prepared under the same conditions as D–A without the polymer network procedure.

size distribution ranging from 30 to 160 nm and average particle size of 100 nm. The X-ray diffraction patterns shown in Fig. 3 confirmed that both samples of D–A and C–A were pure zeolite A structure, and that the polymer network barrier method has no effect on the zeolite A nanocrystals. $N_2$ adsorption–desorption measurements on the directly calcined and $Na^+$ exchanged samples (Fig. 4) show a sharp adsorption step at low relative pressure signifying the filling of micropores. The hysteresis loop at high relative pressures ($>0.9$) is a consequence of $N_2$ filling the large mesopores that are associated with loose packing of dispersible zeolite A nanocrystals.[10] The micropore volume of the directly calcined sample without $Na^+$ exchange is determined to be 0.30 $cm^3\ g^{-1}$, and the Brunaer–Emmett–Teller (BET) surface area is calculated to be 704 $m^2\ g^{-1}$. After $Na^+$ exchange, the micropore volume and BET surface area drop to 0.18 $cm^3\ g^{-1}$ and 485 $m^2\ g^{-1}$ for D–A, and 0.19 $cm^3\ g^{-1}$ and 497 $m^2\ g^{-1}$ for C–A, respectively. Apparently, results for D–A and C–A are comparable, indicating that sodium exchange is equally effective with or without using the polymer network barrier. However, the micropore volume after $Na^+$ exchange did not decrease to zero like true 4A crystals would do possibly because the A crystals had a Si : Al ratio higher than 1 due to use of TMA in the synthesis.[19] This is further supported by elemental analysis results showing that the Na : Si : Al molar ratio of the sample changes from 0.7 : 1.6 : 1 for the as-synthesized sample to 0.8 : 1.6 : 1 after sodium ion-exchange. It is well known that true zeolite 4A has a Na : Si : Al molar ratio of 1 : 1 : 1. Based on elemental analysis results, the composition of as-synthesized zeolite A nanocrystals may be expressed as 0.3 $(TMA)_2O$ : $0.7Na_2O$ : $3.2SiO_2$ : $Al_2O_3$ (in anhydrous form). During calcination, the weight loss can be calculated to be 12.7% due to $TMA^+$ decomposition. The TG analysis result of the as-synthesized sample is shown in Fig. 5. The weight loss of template removal is *ca.* 12.3%, which is consistent with that based on elemental analysis.

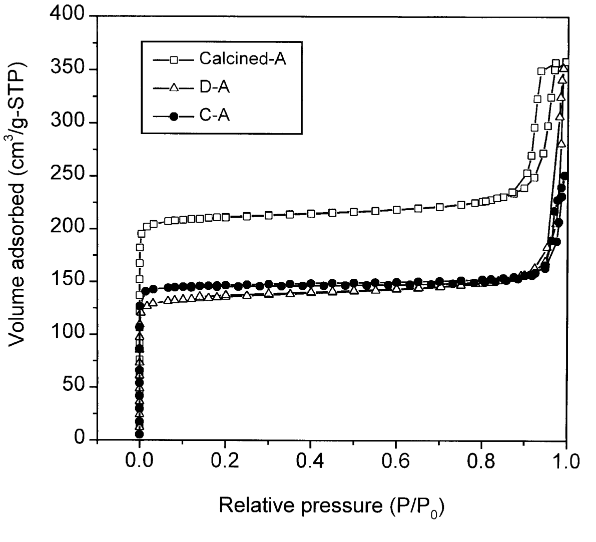

**Fig. 4** $N_2$ adsorption–desorption isotherms of zeolite A nanocrystals. Sample D–A was prepared by polymer network and sodium exchange; sample C–A was prepared under the same conditions as D–A without the polymer network procedure. The sample Calcined-A was obtained by calcination without sodium exchange.

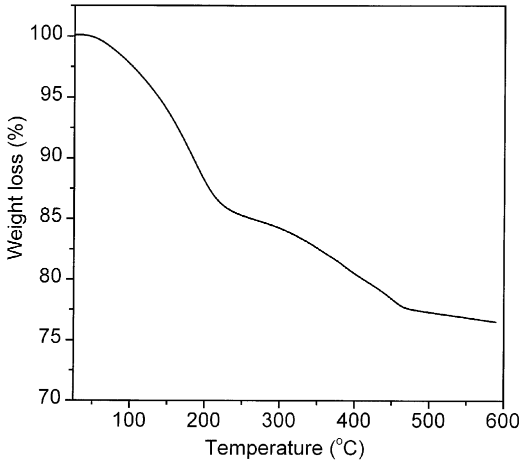

**Fig. 5** TG analysis result of the as-synthesized zeolite A nanocrystals.

## 3.2. Polysulfone–zeolite A nanocomposite membranes

The polysulfone–zeolite A nanocomposite membranes obtained were cloudy white and semitransparent. It was found that zeolite loading has a significant influence on the uniformity of the membrane. At 15 and 25 wt% loading, the nanocomposite membranes (referred to as PSF-A-15, PSF-A-25) were homogeneous. SEM images of the PSF-A-25 membrane show that zeolite A nanocrystals are well dispersed in the polysulfone matrix (Fig. 6a,b), and the membrane has a very smooth surface (Fig. 6b). At high magnification of SEM (Fig. 6a, inset), no voids between the nanocrystal and polysulfone were observed, suggesting good zeolite–polymer contact. However, at a zeolite loading of 30 wt% or higher, the composite membrane seems phase-separated (Fig. 6c), and uniform composite membranes were not obtained. This is probably caused by shrinkage stress of the polymer matrix due to solvent removal. High zeolite A nanocrystal loading could generate significant stress because of rigid polysulfone chains and the agglomeration tendency of the nanocrystals.

The polysulfone and polysulfone–zeolite A nanocomposite membranes were tested for air ($O_2$–$N_2$ mixture) separation. Air separation results of PSF, PSF-A-15 and PSF-A-25 membranes are summarized in Table 1. The $O_2$ permeability and $O_2/N_2$ selectivity of the plain polysulfone membrane are comparable to the data reported in the literature.[2,11,13] The $O_2/N_2$ selectivities of polysulfone–zeolite A nanocomposite membranes are superior to that of the plain polysulfone membrane. The observed selectivity increase is consistent with theoretical predictions. However, the $O_2$ permeability somewhat increases with zeolite A loading, which is opposite to the theoretical prediction.[4] There are experimental data showing that the

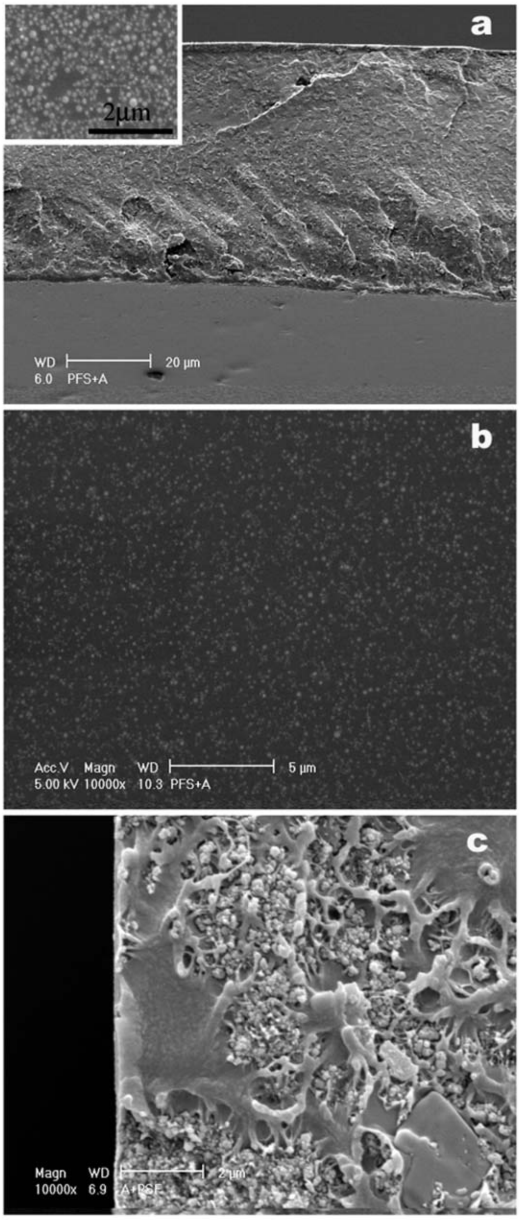

**Fig. 6** SEM images of polysulfone–zeolite A nanocomposite membranes. (a,b) 25% zeolite A loading. (a) Cross-sectional view, inset: cross-section at high magnification. (b) Top view. (c) 30% Zeolite A loading, cross-sectional view.

**Table 1** Air separation results at room temperature of polysulfone and polysulfone–zeolite A nanocomposite membranes

| | Permeability/Barrer | | |
|---|---|---|---|
| | $O_2$ | $N_2$ | $O_2/N_2$ selectivity |
| Polysulfone | 1.3 | 0.22 | 5.9 |
| PSF-A-15 | 1.5 | 0.23 | 6.4 |
| PSF-4A-25 | 1.8 | 0.23 | 7.7 |

permeability for polyethersulfone–zeolite A membranes decreased at certain zeolite loadings (16, 30%) while selectivity was enhanced.[20] It is noted, however, that zeolite A nanocrystals (not micron-sized) are used in this study. The nano-sized particles may alter polymer chain packing in a way different to the large zeolite particles, which, in turn, may improve separation properties without introducing selectivity-destroying defects.[21] More studies are under way on the interfacial interactions between the dispersible zeolite A nanocrystal and polysulfone in order to increase zeolite A nanocrystal loading. The fabrication process for the composite membrane is still being optimized to improve gas separation properties. This approach could be a general one for making polymer–zeolite nanocomposite materials for many applications such as gas separation and fuel cell membranes. In particular, the method described here allows fabrication of asymmetric hollow fibers of composite membranes with a thin selective layer.

## Conclusions

A process strategy for incorporating zeolite nanocrystals into a polymer matrix with homogeneous nanocrystal dispersion is demonstrated. Zeolite A nanocrystals with an average particle size of 100 nm and good dispersibility have been synthesized. Homogeneous polysulfone–zeolite A nanocomposite membrane with up to 25 wt% zeolite nanocrystal loading (PSF-A-25) have been successfully prepared. Addition of 25 wt% zeolite A nanocrystals into polysulfone increases the $O_2/N_2$ selectivity and $O_2$ permeability from 5.9 to 7.7, and from 1.3 to 1.8 Barrers, respectively. The approach for incorporation of dispersible zeolite nanocrystals into a polymer matrix is promising for making polymer–zeolite nanocomposites although the fabrication parameters need to be optimized.

## Acknowledgements

This work was supported in part by the California Energy Commission, Riverside Public Utilities, UC-SMART, AMD, US-EPA, and UC-TSR&TP.

## References

1 R. W. Baker, *Ind. Eng. Chem. Res.*, 2002, **41**, 1389.
2 L. M. Robeson, *Curr. Opin. Solid State Mater.*, 1999, **4**, 549.
3 W. J. Koros and R. Mahajan, *J. Membr. Sci.*, 2000, **175**, 181.
4 C. M. Zimmerman, A. Singh and W. J. Koros, *J. Membr. Sci.*, 1997, **137**, 145.
5 R. Mahajan and W. J. Koros, *Ind. Eng. Chem. Res.*, 2000, **39**, 2692.
6 B. J. Schoeman, J. Sterte and J. E. Otterstedt, *Zeolites*, 1994, **14**, 110.
7 M. A. Camblor, A. Mifsud and J. Perez-Pariente, *Zeolites*, 1991, **11**, 792.
8 L. M. Huang, Z. B. Wang, J. Y Sun, L. Miao, Q. Z. Li, Y. S. Yan and D. Y. Zhao, *J. Am. Chem. Soc.*, 2000, **122**, 3530.
9 B. Moermans, W. De Beuckelaer, I. F .J. Vankelecom, R. Ravishankar, J. A. Martens and P. A. Jacobs, *Chem. Commun.*, 2000, 2467.
10 H. T. Wang, Z. B. Wang and Y. S. Yan, *Chem. Commun.*, 2000, 2333.
11 A. F. Ismail, I. R. Dunkin, S. L. Gallivan and S. J. Shilton, *Polymer*, 1999, **40**, 6499.
12 C. Macht and G. Hinrichsen, *Sep. Purif. Technol.*, 2001, **22-23**, 247.
13 I. Pinnau and W. J. Koros, *J. Appl. Polym. Sci.*, 1991, **43**, 1491.
14 T. Brar, P. France and P. G. Smirniotis, *Ind. Eng. Chem. Res.*, 2001, **40**, 1133.
15 R. M. Barrer, P. J. Denny and E. M. Flanigen, *US Pat.* 3 306 922, 1967.
16 S. Mintova, N. H. Olson, V. Valtchev and T. Bein, *Science*, 1999, **283**, 958.
17 G. S. Zhu, S. L. Qiu, J. H. Yu, Y. Sakamoto, F. S. Xiao, S. R. Xu and O. Terasaki, *Chem. Mater.*, 1998, **10**, 1483.
18 L. C. Boudreau, J. A. Kuck and M. Tsapatsis, *J. Membr. Sci.*, 1999, **152**, 41.
19 D. W. Breck, W. G. Eversole, R. M. Milton, T. B. Reed and T. L. Thomas, *J. Am. Chem. Soc.*, 1956, **78**, 5963.
20 M. G. Suer, N. Bac and L. Yilmaz, *J. Membr. Sci.*, 1994, **91**, 77.
21 T. C. Merkel, B. D. Freeman, R. J. Spontak, Z. He, I. Pinnau, P. Meakin and A. J. Hill, *Science*, 2002, **296**, 519.